INL/CON-05-00028
PREPRINT

Natural Convection Heat Transfer Experiment In A Hemispherical Pool

ICAPP '05

Seung Dong Lee
Hyoung M. Son
Kune Y. Suh
Joy L. Rempe
F. Bill Cheung
Sang B. Kim

May 2005

The INL is a
U.S. Department of Energy
National Laboratory
operated by
Battelle Energy Alliance

Proceedings of ICAPP '05
Seoul, KOREA, May 15-19, 2005
Paper 5577

Natural Convection Heat Transfer Experiment in a Hemispherical Pool

Seung Dong Lee, Hyoung M. Son, Kune Y. Suh*
Seoul National University
San 56-1 Sillim-dong, Gwanak-gu, Seoul, 151-742, Korea
**Tel: 82-2-880-8324, Fax: 82-2-889-2688, Email: kysuh@snu.ac.kr*

Joy L. Rempe
Idaho National Engineering & Environmental Laboratory
P.O. Box 1625, Idaho Falls, ID 83415, USA

F. Bill Cheung
The Pennsylvania State University
304 Reber Building, University Park, PA 16802, USA

Sang B. Kim
Korea Atomic Energy Research Institute
P.O. Box 105, Yusong, Daejeon, 305-6008, Korea

Abstract – *Natural convection plays an important role in determining the thermal load from molten core accumulated in the reactor vessel lower head during a severe accident. Several numerical and experimental programs were conducted to study the heat transfer in the molten pool. Previous investigations were mostly related to the rectangular and semicircular pools. Except for COPO, UCLA, ACOPO, and BALI, previous investigations suffer from inadequate representation of high modified Rayleigh number (Ra') in the hemispherical pool that may be formed in the reactor core and lower plenum. Thus, experimental work is conducted utilizing SIGMA SP (Simulant Internal Gravitated Material Apparatus Spherical Pool) producing high Ra' turbulent natural convection in a hemispherical pool up to 5.3×10^{11}. The heating method has already been tested in SIGMA CP (Circular Pool). Six thin cable-type heaters, each with a diameter of 6 mm, are employed to simulate internal heating in the pool. They are uniformly distributed in the hemispherical pool to supply a maximum of 7.8 kW power to the pool. SIGMA SP has the inner and outer diameters of 500 mm and 520 mm, respectively. The upper flat plate and the curved wall of pool, with a 10 mm thick stainless steel plate, are cooled by a regulated water loop. A water-cooling system is used to maintain the temperature of water surrounding the test section nearly constant with time. This study focuses on quantifying the directional heat losses, angular heat flux distribution, and temperature distribution inside the molten pool.*

I. INTRODUCTION

During a severe accident, the molten core can relocate to the lower plenum of the reactor vessel and form a hemispherical pool. Should there be no effective cooling mechanisms, the core debris may heat up on account of decay power. The molten core material will threaten the structural and thermal integrity of the reactor vessel. The extent and urgency of this threat depend primarily on the intensity of the internal heat sources and the consequent distribution of heat fluxes on the vessel wall in contact with the molten core material. Although the modified Rayleigh number (Ra') in this experiment was less than that of the molten core in the rage of 10^{17} by several orders of magnitude, the results certainly shed light on the basic natural convection phenomena in a volumetrically heated hemispherical pool.

II. LITERATURE SURVEY

II.A. Previous Numerical and Experimental Studies

Several numerical and experimental investigations were performed to study heat transfer in the spherical pool.

Tests were conducted on heat transfer from internally heated $ZnSO_4$-H_2O spherical pools to curved surfaces with free upper surface by Gabor et al.[1] The lower spherical surface was cooled and served as one of the electrodes. Three different sizes of copper spherical containers were used: 240, 280, and 320 mm in diameter. A copper disk in the center placed near the pool free surface, served as the other electrode. This experimental method for internal heat generation does not result in uniform heat generation throughout the pool since the electrical current density decreases radially from the center electrode to the wall. The average heat transfer coefficients for $2\times10^{10}<Ra'<2\times10^{11}$ and $0.5<L/R<1.0$ were correlated as

$$Nu_{dn} = 0.55\ Ra'^{-0.15}(L/R)^{1.1} \quad (1)$$

They concluded that the maximum temperature occurred in the middle of the upper pool surface, which was open to the atmosphere.

Asfia and Dhir[2] conducted experiments to examine natural convection heat transfer in an internally heated partially filled hemispherical pool with external cooling. Microwave heating by 750W magnetron was used as the heat source. In this method, test fluid was R-113 only. Other fluids showed significant non-uniformities. The average heat transfer coefficients for $2\times10^{10}<Ra'<1.1\times10^{14}$ and $0.26<L/R<1.0$ were correlated as

$$Nu_{dn} = 0.54\ Ra'^{-0.2}(L/R)^{0.25} \quad (2)$$

The results showed that the heat transfer coefficient was lowest at the bottom and then increased along the hemispherical segment. The ratio of maximum to minimum heat transfer coefficient can be as high as 20, while the ratio of maximum to average heat transfer coefficient can be as high as 2.5.

Theofanous et al.[3] and Theofanous and Angelini[4] used the ACOPO test apparatus to simulate natural convection heat transfer from the volumetrically heated pools at a half scale reactor lower head for Ra′ up to 10^{16}. In contrast to the previous experiment, ACOPO used the "cool-down method" to get the effect of internal heating. The average heat transfer coefficients for $1\times10^{12}<Ra'<2\times10^{16}$ were correlated as

$$Nu_{up} = 1.95\ Ra'^{-0.18} \quad (3)$$
$$Nu_{dn} = 0.3\ Ra'^{-0.22} \quad (4)$$

The results indicated that the externally and internally driven natural convection problems are exactly analogous; the ACOPO data trend is towards reaching the 1/3-law; and an unambiguous Prandtl number dependency of 0.084 exists in both external and internal problems.

Lee[5] carried out the numerical study of high Ra′ turbulent natural convection of molten core material in the hemispherical pool. A computational code HITNIS was developed. The HITNIS calculational results were compared with the mini-ACOPO experimental data for $2\times10^{13}<Ra'<7\times10^{14}$. The calculated average Nusselt numbers showed reasonably good agreement with the mini-ACOPO data along the lower curved boundary but a maximum deviation of 15% at the upper flat boundary. The average heat transfer coefficients were correlated as

$$Nu_{up} = 0.2692\ Ra'^{-0.2364} \pm 22 \quad (5)$$
$$Nu_{dn} = 0.0916\ Ra'^{-0.2534} \pm 42 \quad (6)$$

The SIGMA (Simulant Internal Gravitated Material Apparatus) tests are concerned with a high Ra′ turbulent natural convection in a molten pool. The internal heating method is employed in the test by using cable-type heaters. The main results include the heat split fraction, angular heat flux distribution, and temperature distribution inside the molten pool.

Previous investigations suffer from lack of properly representing a molten core material behavior in the reactor vessel lower plenum involving specific conditions such as high Ra′, turbulent boundary layers, a low height-to-diameter ratio, and a spherical geometry. Thus, extrapolations to different geometries and convection conditions must be considered with reservation. Further, whereas in many previous studies only the average heat transfer from liquid to the walls has been correlated, the heat flux profiles and their peak values are also needed for safety assessment concerning the external reactor vessel cooling.

II.B. Dimensionless Parameters

The spatial and temporal variation of heat flux on the pool wall boundaries and the pool superheat characteristics depend strongly on the natural convection flow pattern inside the molten pool. The natural convection heat transfer involving internal heat generation is represented by Ra′ which quantifies the internal heat source and hence the strength of the buoyancy force. Natural or free convection phenomena can be scaled in terms of the Grashof number (Gr), the Prandtl number (Pr), and additionally, the Dammkohler number (Da) in the presence of volumetric heat sources. The dimensionless numbers are defined as

$$Gr = \frac{g\beta\Delta TL^3}{\nu^2};\ Pr = \frac{\nu}{\alpha};\ Da = \frac{QL^2}{k\Delta T} \quad (7)$$

The Rayleigh number (Ra) can be used to characterize the heat transfer in natural or free convection problems, including those involving internal heat sources or external

heating such as heating from below. This dimensionless number is defined as

$$Ra = Gr\,Pr = \frac{g\beta\Delta TL^3}{\alpha\nu};\ \alpha = \frac{\kappa}{\rho C_p};\ \nu = \frac{\mu}{\rho} \qquad (8)$$

The preceding equation relates the buoyancy and viscous forces, which are linearly related via the factor, Gr/Re, but other dependencies are also present. Ra′ is germane to free or natural convection problems with internal heat sources, and it is defined as

$$Ra' = RaDa = Gr\,Pr\,Da = \frac{g\beta QL^5}{\alpha\nu\kappa} \qquad (9)$$

In general, the natural convection heat transfer phenomena involving the internal heat generation are adequately represented by such dimensionless parameters as Ra′ and Pr, and physical dimensions of the pool. For the natural convection phenomena involved in reactor vessel molten core material flow, the predominant driving force for heat transport processes is the internal heating from the decay heat, while the conduction effects are relatively small. Thus, the heat transfer rates are primarily governed by Ra′. The average Nusselt number has been correlated reasonably well by the following relation, which incorporates the dependence on Ra′ and the geometric parameter, L/R.

$$Nu = C \cdot Ra'^{m}\left(\frac{L}{R}\right)^{m} = \frac{hL}{\kappa} \qquad (10)$$

The Nusselt number is equal to the dimensionless temperature gradient at the surface providing a measure of the convection heat transfer occurring at the surface. The constant value of L/R=1 corresponds to the situation where the vessel bottom head is filled up. For this case Equation (10) reduces to the following simplified power law form for the Nusselt number as a function of Ra′

$$Nu = C \cdot Ra'^{m} \qquad (11)$$

For low values of Ra′, the turbulence intensity is small and the turbulent or eddy viscosity is negligible in comparison with the molecular viscosity. Such flows can be characterized as laminar and, furthermore, they would be steady if the internal heat source and boundary conditions vary slowly over the time scale of interest. However, the flow is characterized as turbulent and unsteady for large values of Ra′, at least in domains of vigorous mixing and high turbulent intensity, and the molecular viscosity is small in relation to the eddy viscosity. Regions of laminar, transition and turbulent flow may coexist in the pool according to the thermal stratification of the molten core material.

III. EXPERIMENT

While a number of investigations have dealt with the rectangular and semicircular pools, relatively few test data exist for the hemispherical pool. SIGMA SP considers the hemispherical pool employing the same internal heating method as was already used in SIGMA CP for a circular pool. The radius of the test section is 250 mm as depicted schematically in Figure 1.

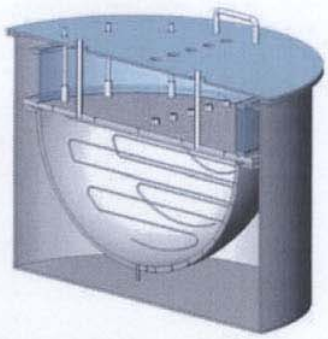

Fig. 1. Schematic of the SIGMA SP test section

Figure 2 shows the detailed drawing of the SIGMA SP test section in which the internal heaters are embedded. The pool's upper flat wall and hemispherical curved wall, with a 10 mm thick stainless steel plate, are cooled by a regulated water loop. A water-cooling system is used to maintain the temperature of water surrounding the test section constant with time. During the period of two hours, the boundary temperature fluctuation was maintained within 1 .

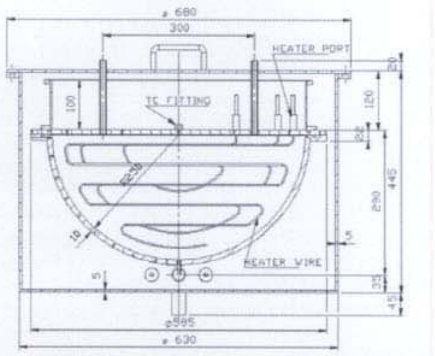

Fig. 2. Detailed drawing of the SIGMA SP test section

Figure 3 illustrates the location of the thermocouples in the pool.

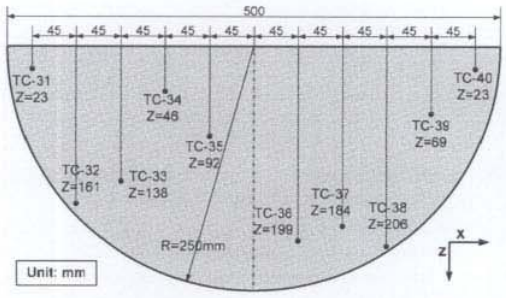

Fig. 3. Thermocouple location in the test pool

Figure 4 is the conceptual diagram of the SIGMA SP water test. The SIGMA SP water test was conducted to check on performance of the water cooling circuit, cable-type heaters, thermocouples and the data acquisition system (DAS) against available natural convection data.

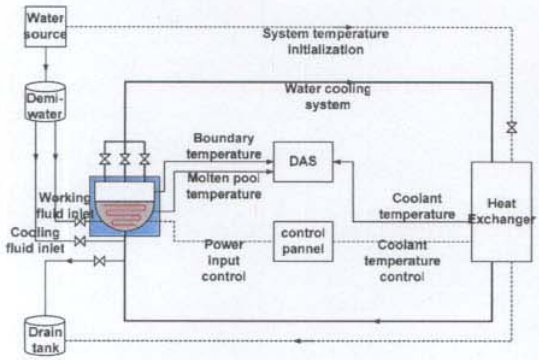

Fig. 4. Schematic diagram of the SIGMA SP test loop

III.A. Heating Method

The internal heater method had already been used by Kolb et al.[6], and Lee and Suh[7]. However, both test sections were of a two-dimensional circular pool. Thus, the SIGMA SP test is the first to use the internal heaters in a hemispherical pool. Six thin cable-type heaters, with a diameter of 6 mm and a pair of the length of 1980 mm, 1760 mm, and 640 mm, respectively, are used to simulate internal heating in the pool. The difference between heaters was 80 mm. They are uniformly distributed in the apparatus and thus can supply a maximum of 7.8 kW power to the pool yielding Ra′ as high as 2.3×10^{13}. Uniformity of the heat generation rate is one of the most important conditions in the SIGMA SP test. Figure 5 presents the temperature transient rate at different locations.

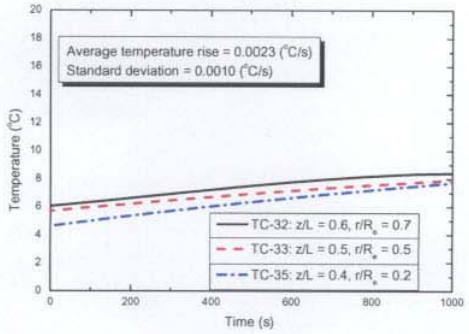

Fig. 5. Temperature rise rate at different locations

III.B. Experimental Procedure

Thermocouple locations in the SIGMA SP apparatus are shown in Figure 6 and Table 1. After the water leakage test, the thermocouples were calibrated by the ISOTECH Temperature Reference Unit Model 740. Forty-two T-type thermocouples are submerged in a constant temperature pool sequentially. The data were compared with the temperature reading from a separate thermometer.

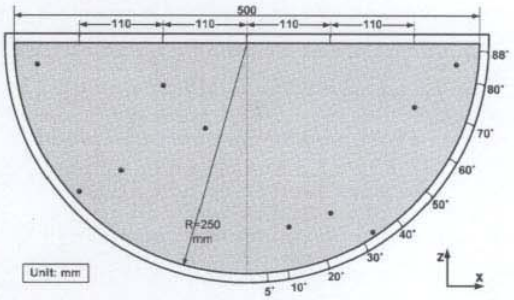

Fig. 6. Thermocouple location on the test wall

The DAS bias error was thus calibrated so as to minimize the measurement error. Calibration curves were then drawn for each thermocouple. The relative error in reading from a T-type thermocouple was determined from these curves. All the thermocouples were placed in designated spots after calibration.

In this experiment, the 1 mm diameter thermocouples are utilized to calculate the heat flux for the upper and lower walls. The thermocouple hole is 1.2 mm in diameter, and 2 and 9 mm in depth, respectively, in pairs on the 10 mm stainless steel wall.

Table 1 presents the location of each thermocouple. Twenty thermocouples were mounted on the surface of the stainless steel wall along the centerline and through the test section from the bottom (θ=5°) to just below the equator (θ=88°) to obtain the azimuthal heat flux. Because of the drain valve at the bottom, location of the azimuthal thermocouple started at 5°. Ten thermocouples were installed at the upper plate to obtain the upper heat flux. Another ten thermocouples were submerged in the test pool to find the fluid temperature. Two thermocouples were placed in the external tank to determine the boundary temperature.

Table 1. Thermocouple location in the apparatus

	No.	Location	Note
Pool	10	-225, -180, -135, -90, -45, 45, 90, 135, 180, 225	
Horizontal	5	-220, -110, 0, 110, 220	z = 251
Horizontal	5	-219, -109, 1, 111, 221	z = 258
Azimuthal (stainless steel)	10	5°, 10°, 20°, 30°, 40°, 50°, 60°, 70°, 80°, 88°	R = 251
Azimuthal (stainless steel)	10	5°, 10°, 20°, 30°, 40°, 50°, 60°, 70°, 80°, 88°	R = 258
Boundary	2	Upper pool / Lower pool	
Total	42		unit: mm

Initially the temperatures of the working fluid in the test section and water cooling system reached a steady state. The water cooling system maintains the upper and lower boundaries isothermal. A performance test of this water cooling system showed a temperature difference within 0.5 spanning 5 to 80 . The pool was then allowed to heat up. The DAS was initially adjusted to record the temperature every second to check on the uniformity of the heat generating rate.

III.C. Test Matrix

Tests were conducted using two different fluids: water (Pr~6.5) and air (Pr~0.7). The difference in temperatures between the inlet and outlet is less than 1 . Thus the upper flat surface and lower hemispherical surface are isothermal. The test matrix is summarized in Table 2.

Table 2. Test matrix with varying input power

Air	Power (W/m^3)	Water	Power (W/m^3)
Case-1A	4.3	Case-1W	4.0
Case-2A	15.1	Case-2W	16.4
Case-3A	38.6	Case-3W	64.3
Case-4A	63.7	Case-4W	146.7
Case-5A	102.1	Case-5W	262.5
Case-6A	142.8	Case-6W	402.0
Case-7A	200.4	Case-7W	573.1
Case-8A	269.0	Case-8W	3899.0
Case-9A	338.8	Case-9W	24371.0
Case-10A	408.5	Case-10W	62391.0

IV. RESULTS AND DISCUSSION

The stainless steel inner and outer surface temperatures were measured to determine the upper heat flux. From these data the local heat flux can be calculated as

$$q''_{loc} = -\kappa \frac{(T_{loc} - T_w)}{dx} \tag{12}$$

The average heat flux then takes the form

$$q''_{avg} = \int q''_{loc}\, dA / \int dA \tag{13}$$

$$A = \int_{R_1}^{R_2} 2\pi r dr = \pi(R_2^2 - R_1^2) \tag{14}$$

In case of lower heat flux

$$A = \int_{\theta_2}^{\theta_1} 2\pi R^2 \sin\theta d\theta = 2\pi R^2(\cos\theta_1 - \cos\theta_2) \tag{15}$$

The average heat transfer coefficient is then obtained from

$$h_{avg} = \frac{q''_{avg}}{(T_{max} - T_w)} \tag{16}$$

Figure 7 shows the temperature profile in the pool. The steady state is defined such that the temperature fluctuation stays within 0.5 over the period of 1,000 s. During the air experiment, a steady state is reached at 3,500 s. In contrast, during the water test, a steady state is attained at 14,000 s, four times that of air. The difference in the steady state points may be explained in terms of specific heat. The specific heats of water and air are 4.2 and 1.0 kJ/kgK in the temperature range of this experiment,

respectively. In both cases, as the input power is increased, the steady state point is delayed.

The ratio of the local heat flux to the average heat flux on the upper surface is presented in Figure 8. The ratio was close to unity at five locations in case of water. Though this graph is related to water, air case yielded the same results. The results followed closely the COPO II experimental values.

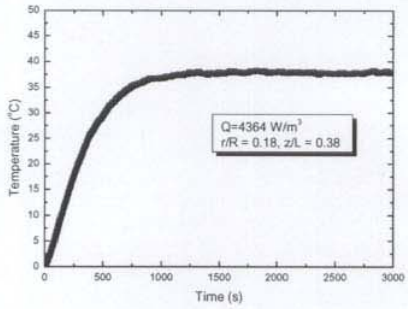

(a) air

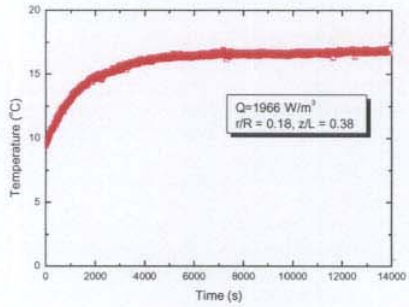

(b) water

Fig. 7. Steady state for the immersed thermocouple

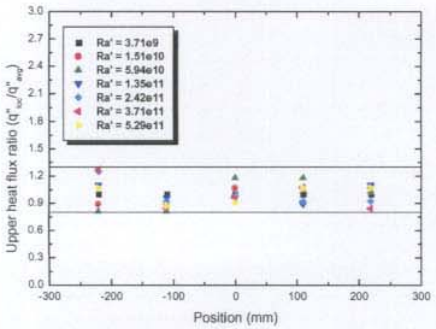

Fig. 8. Heat flux distribution on the upper wall

Figure 9 shows that the ratio of the local to average heat transfer coefficient. The heat transfer coefficients were normalized to the average heat transfer coefficients on the curved wall. In this graph the result of Asfia and Dhir[2] was compared with Case-1A in this study.

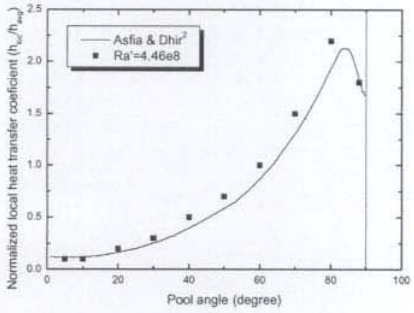

Fig. 9. Ratio of local to average downward heat transfer coefficient

As the pool angle increases, the ratio of the local to average heat transfer coefficient also increases except in the vicinity of the equator. In this region not only the downward but also the upward heat transfers increase. Thus, the maximum ratio of the heat transfer coefficient is around 80 . Also, the ratio of heat transfer coefficient at 88 is between 70 and 80 . The water cases yielded similar results.

Figure 10 demonstrates the downward Nusselt number given Ra′. The results were similar to Asfia and Dhir[2] and Theofanous et al.[3] above the value of $Ra' = 10^{10}$. Their investigations were implemented in range of $10^{11}<Ra'<10^{14}$. Thus, it is difficult to make a direct comparison. So as to compare against the previous results, the scale of Ra′ was revised.

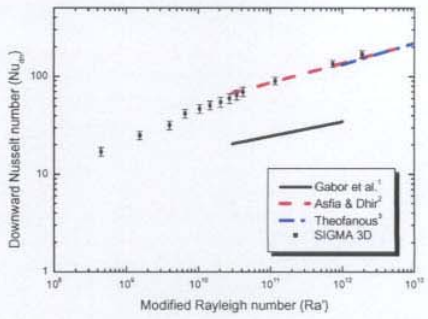

Fig. 10. Average downward Nusselt number

The uncertainties in the thermophysical properties and geometrical factors produced an experimental uncertainty of 2 % in Ra′. The power output per unit volume by the voltmeter readings produced an uncertainty of 3 % in Ra′. Over the period of two hours, the variation in the boundary water temperature was neglected since the temperature differences stayed within 0.5 . The total experimental uncertainty in computed values of the Nusselt number was determined as 10 %.

V. CONCLUSIONS

The results demonstrated practicability of the cable-type heating in simulating the volumetric heat source in the hemispherical pool. Although maximum input power was 7.8 kW, the input power in SIGMA SP was limited to 6.2 kW so as to prevent water from boiling. The uniform heat generation rate was identified. Use of the simulant fluid such as air and water requires particular care to reproduce the same physical behavior of the natural convection heat transfer in the molten pool. There persist difficulties to transpose results to the reactor scale such as Ra′. Major findings from this study may be summarized as follows.

(1) Steady state point during the water experiment is about four times that for air due mostly to differing specific heats.
(2) The upper heat flux ratio approximated unity at all locations in the water test. The air test yielded the same results.
(3) As the pool angle increases, ratio of the local to average heat transfer coefficients also increases except in the vicinity of the equator.
(4) The downward Nusselt number was similar to the correlations by Asfia and Dhir[2] and Theofanous et al.[3] above the value of Ra′ 10^{10}.

NOMENCLATURE

A	area	[m^2]
C	coefficient in Equations (10) and (11)	
C_p	specific heat	[J/kg·K]
Da	Dammkohler number	
g	gravitational acceleration	[m/s^2]
Gr	Grashof number	
h	heat transfer coefficient	[W/m^2·K]
k	thermal conductivity	[W/m·K]
L	pool height	[m]
Pr	Prandtl number	
q''	heat flux	[W/m^2]
Q	heat generation rate	[W/m^3]
R	radius	[m]
r	radius	[m]
Ra	Rayleigh number	
Ra'	modified Rayleigh number	
T	temperature difference	[K]
x	distance	[m]
z	height	

Greek Letters

α	thermal diffusivity	[m^2/s]
β	thermal expansion coefficient	[K^{-1}]
μ	dynamic viscosity	[$N·s/m^2$]
ν	kinematic viscosity	[m^2/s]
θ	angle	[degree]
ρ	density	[kg/m^3]
Δ	difference	

Subscript

avg	average
dn	downward
loc	local
max	maximum pool temperature
up	upward
w	boundary wall
1	small value
2	large value

Superscript

m	exponent in Equation (10)
n	exponent in Equations (10) and (11)

ACKNOWLEDGMENTS

This work was performed under the auspices of the Korean Ministry of Science and Technology (contract number M20112 000001-01B0300-00210) and U.S. Department of Energy (contract number DE-ACO7-991D13727) as an International Nuclear Energy Research Initiative project awarded to the Seoul National University and the Idaho National Engineering and Environmental Laboratory in collaboration with the Korea Atomic Energy Research Institute and the Pennsylvania State University.

REFERENCES

1. J. D. GABOR, P. G. ELLISON and J. C. CASSULO, "Heat Transfer from Internally Heated Hemispherical Pools," *Proceedings of 19th National Heat Transfer Conference*, ASME, Orlando, FL, USA, July (1980).

2. F. J. ASFIA and V. K. DHIR, "An Experimental Study of Natural Convection in a Volumetrically Heated Spherical Pool Bounded on Top with a Rigid Wall," *Nuclear Engineering and Design*, **163**, 333-348 (1996).

3. T. G. THEOFANOUS, M. MAGURIE, S. ANGELINI and T. SALMASSI, "The First Results from the

ACOPO Experiment," *Nuclear Engineering and Design*, **169**, 49-57 (1997).

4. T. G. THEOFANOUS and S. ANGELINI, "Natural Convection for In-vessel Retention at Prototypic Rayleigh Numbers," *Nuclear Engineering and Design*, **200**, 1-9 (2000).

5. H. D. LEE, "Study of High Rayleigh Number Turbulent Natural Convection of Molten Corium in the Hemispherical Geometry," *Ph.D. Dissertation*, Department of Nuclear Engineering, Seoul National University, Seoul, Korea (1999).

6. G. KOLB, S. A. THEERTHAN and B. R. SEHGAL, "Experiments on In-vessel Melt Pool Formation and Convection with $NaNO_3$-KNO_3 Salt Mixture as Melt Simulant," *Proceedings of International Conference on Nuclear Engineering, ICONE-8639*, Baltimore, MD, USA, April 2-6 (2000).

7. S. D. LEE and K. Y. SUH, "Natural Convection Heat Transfer in Two-Dimensional Semicircular Slice Pool," *Journal of Nuclear Science and Technology*, **40**, *10*, 775-782 (2003).